

Coherent and incoherent space charge resonance effects

Ingo Hofmann

*Technische Universität Darmstadt, Schlossgartenstr. 8, 64289 Darmstadt, Germany and
GSI Helmholtzzentrum für Schwerionenforschung GmbH, Planckstr. 1, 64291 Darmstadt, Germany**

The question of interplay of coherent and incoherent space charge driven resonances and of their Landau damping has found some interest in beam dynamics of modern high-intensity synchrotrons. We revisit the theoretical and simulation models describing coherent half-integer parametric resonances, analyze their Landau damping in 2D beams on the basis of simulated tune spectra and conclude that above second order (envelope modes) they play no role in realistic, Gaussian-like beam models. We also analyze incoherent resonance effects in the beam core regions and find that their role has been underestimated in part of the literature, in particular with regard to the very long-term beam evolution as in synchrotrons. We conclude that for such time scales more careful analysis of realistic simulation models is needed to support synchrotron design and evaluation of experiments.

I. INTRODUCTION

In linear accelerators space charge resonance effects are known to occur at sufficiently high intensity and under structure resonance conditions. Their effect is often not evident due to limited length; nonetheless satisfactory comparison of experimental data with theoretical predictions was reported a few years ago by Groening [1, 2].

In circular accelerators the usually very large number of turns and the presence of external nonlinearities besides space charge lead to additional difficulties, which make progress more challenging. While coherent effects in impedance driven instabilities are a common topic, the role of coherent effects in transverse resonances is not yet adequately explored. Magnet error induced resonances with space charge effects in synchrotrons have been observed in detailed studies at the GSI and CERN synchrotrons [3–5]. Relatively satisfactory match between experiment and simulation models has been achieved in these studies, but important issues are still pending. The simplified simulation models, for example, have relied on so-called frozen space charge models (FSM), which lack selfconsistency and would suppress any kind of coherent response - if excited by whatever mechanism. The extent, to which it helps to update the rms emittance is yet unclear and requires benchmarking with selfconsistent codes.

In the following some aspects on the interplay of incoherent and coherent effects are presented. Section II reviews some historical and theoretical respectively experimental aspects of coherent frequency shifts. In Section III we discuss the so-called half-integer (parametric) coherent resonances including their Landau damping. Section IV is dedicated to incoherent versus coherent resonance effects, Section V to a comparison with experiments and Section VI attempts an outlook.

II. COHERENT RESONANCE EFFECTS

The question of coherent resonant effects was first brought up by Smith [6] who pointed out - on the basis of envelope equations - that gradient error driven resonances should occur at the resonance condition for the coherent tune rather than the incoherent one. Later, his student Sacherer [7] derived conditions for higher order magnet driven resonances and their respective selfconsistently calculated coherent shifts in a 1D sheet beam model using the linearized Vlasov-Poisson equation.

The subject of coherent resonance effects found little attention in the years to follow. A pioneering selfconsistent simulation study in a synchrotron lattice with half-integer gradient error resonances using different beam distributions, and simulation limited to a few hundred turns, was carried out by Machida in 1991 [8] - with results supporting to some extent the conjecture by Smith.

It is helpful to take a quantitative look at the coherence issue on the second order level. For sufficiently split tunes a straightforward calculation of the envelope mode oscillation frequency by using the rms envelope equations yields the well-known result for the coherently shifted frequency (in “smooth approximation”)

$$\omega = 2(\bar{Q}_{xy} + \frac{3}{8}\Delta\bar{Q}_{xy}), \quad (1)$$

where $\bar{Q}_{xy} \equiv Q_{0xy} - \Delta\bar{Q}_{xy}$ is the incoherent tune and $\Delta\bar{Q}_{xy}$ the space charge tune shift based on KV rms equivalence. Note that the KV-equivalent \bar{Q}_{xy} is to be distinguished from the amplitude dependent Q_{xy} in non-KV beams.

The resulting theoretical coherent resonance condition for the gradient error case is then

$$2(\bar{Q}_{xy} + \frac{3}{8}\Delta\bar{Q}_{xy}) = n, \quad (2)$$

where n is an integer depending on the lattice. Condition Eq. 2 is in contrast with the still widely used second order incoherent resonance condition $2\bar{Q}_{xy} = n$.

* i.hofmann@gsi.de

The predicted intensity advantage under the assumption that only the coherent condition matters is not negligible. The situation is illustrated schematically in Fig. 1 by using the “necktie” diagrams for a 2D Gaussian distribution with a total spread $2\Delta\bar{Q}_{xy}$, and by assuming a gradient error coherent shift as in Eq. 2. The three cases

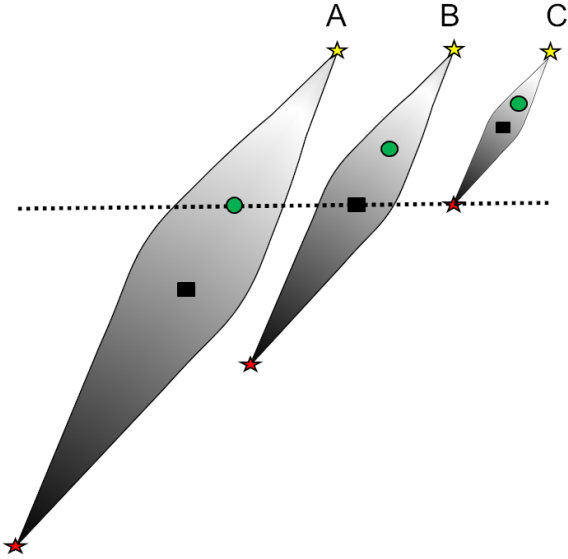


FIG. 1. Schematic comparison of different approaches to resonance diagram “neckties” referring to an assumed Gaussian distribution and a gradient error resonance line (dotted). Indicated are the coherent tune $\omega/2$ (green circle), Q_{0xy} (yellow star), the lower tip of Q_{xy} (red star) and \bar{Q}_{xy} (black square).

depicted in Fig. 1 relate to

1. “incoherent limit” (C) assuming that the full footprint must be above the resonance
2. “coherent limit” (A): only the coherent frequency needs to be above the resonance
3. “rms limit” (B): the rms tune \bar{Q}_{xy} is above the resonance.

Note that the idealized intensity advantage of A compared with C would be a factor 3.2, whereas B relates to a doubling of intensity. Smith was still pointing at the full “coherent advantage” (case A), while the simulation results of Machida have confirmed the less optimistic rms limit - still with an approximate intensity gain of a factor 2. A similar “benefit” was recently reported from simulations for the JPARC Rapid Cycling Synchrotron with the finding that no emittance growth or loss is observed as long as the rms tune stays above the driving resonance condition [9].

In fact, the coherent frequency approach entirely ignores that besides the coherent envelope frequency there is also a spectrum of incoherent single particle frequencies Q_{xy} covering the whole range of frequencies. The question of their role with regard to resonances requires

additional considerations not yet well understood systematically.

The idea of coherent shifts in higher than second order, driven by nonlinear magnet error or structure resonances, is summarized in the analogous smooth approximation expression

$$m(\bar{Q}_{xy} + F_m\Delta\bar{Q}_{xy}) = n. \quad (3)$$

Corresponding coherent shifts from second to fourth order in a 2D beam Vlasov-Poisson model with arbitrary (smooth) focusing and emittance ratios, and under the assumption of no frequency spread, have been derived in the late 1990’s by Hofmann [10] (see also Ref. [11] for detailed examples of F_m). For split focusing they result as: $F_2 = 3/8$, $F_3 = 5/24$ and $F_4 = 35/256$. Note that for still higher order m it can be assumed that the F_m further approach zero.

For our discussion of the role of frequency spread it is helpful to generate different selfconsistent spectral tune distributions Q_{xy} and allocate on them the coherent frequencies according to calculated shifts. This is shown in Fig. 2 comparing a waterbag with a Gaussian distribution for a coasting beam with a working point such that no significant resonance occurs (here $Q_{0x} = 0.158$, $Q_{0y} = 0.206$ and $\Delta\bar{Q}_{xy} = 0.0322$).

These spectra can be used also as initial spectra for any other value of Q_{0y} and $\Delta\bar{Q}_{xy}$, if appropriately shifted and re-scaled in width. The spectra shown here are generated by using the TRACEWIN code [12], for this case with 32.000 particles, transported through a straight FODO latticed over 3000 cells, where the last 2000 cells are used to Fourier transform particle orbits and generate the spectral tune plot. Tunes Q refer to a single FODO cell as fractions of 360° . The location of coherent frequencies

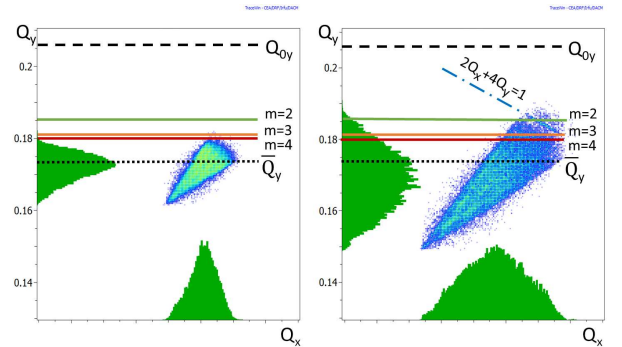


FIG. 2. Spectral distribution of Q_{xy} for 2D waterbag (l.h.s.) and Gaussian (r.h.s.) distributions in a largely resonance-free region. Also shown are locations of expected $m = 2\dots 4$ coherent mode frequencies, furthermore Q_{0y} and \bar{Q}_y ; a weak incoherent coupling resonance $2Q_x + 4Q_y = 1$ exited by the periodical space charge pseudo-dodecapole component of the matched beam is also shown.

has been corrected from the purely theoretical ones by using TRACEWIN simulation results for waterbag beams [13].

Comparing Fig. 2 with Fig. 1 we note that the higher order coherent ω/m would be closer to \bar{Q}_{xy} than the envelope $\omega/2$ (green circle). Hence, the theoretical intensity benefit from the coherent effect shrinks for higher than second order - an argument speaking in favor of the more cautious “rms limit” (B).

A review article at the 1998 Shelter Island Workshop by Baartman [14] once more drew attention to the theoretical predictions of space charge shifted coherent resonance conditions in all orders for magnet error driven resonances (similar to Eq. 3, but using a different notation for F_m). The basis of Eq. 3, however, continued to be largely an analytical-theoretical one. Up to the present day clear benchmarking of the coherent resonance thesis with experimental findings for coasting or bunched beams in circular accelerators is not available.

Therefore, - apparently due to this lack of experimental evidence - the circular accelerator community widely continued to use “necktie” resonance diagrams based on the “incoherent space charge limit”, with the possibly over-cautious requirement that no significant resonance line should intercept the necktie at any point.

In their recent article, Kojima et al. [15] take up a strong position by suggesting that synchrotron resonance charts should be redefined on the basis of coherent effects. However, these conditions have so far been studied in 2D and over a small (few hundred) number of lattice cells only. The real issue for synchrotrons is long-term behavior and the effect of synchrotron motion, which can be expected to enhance the emphasis on incoherent resonance effects - along with Landau damping.

III. HALF-INTEGER (PARAMETRIC) COHERENT RESONANCES AND LANDAU DAMPING

The theoretical concept of coherent resonances discussed in Section II is not limited to the externally driven resonance cases of Eq. 3. In principle, so-called *coherent half-integer parametric resonances* driven by space charge alone and described by a half-integer r.h.s. according to

$$m(\bar{Q}_{xy} + F_m \Delta \bar{Q}_{xy}) = \frac{n}{2}, \quad (4)$$

(with n an odd integer) need to be included as they potentially lead to additional lines in resonance charts. Note that the coherent half-integer modes are essentially different from half-integer or gradient error resonances described by $2\bar{Q}_{xy} = n$, or its coherent extension $2(\bar{Q}_{xy} + F_2 \Delta \bar{Q}_{xy}) = n$.

Historically, these coherent half-integer parametric resonances have been introduced in a selfconsistent 2D Vlasov study in periodic focusing lattices by Hofmann et al. [16]. At that time they were called “180-degree” modes due to the fact that two lattice periods are needed to complete one mode period. The today more commonly

used terminology of “parametric resonances” was later suggested in an analogous 1D sheet beam Vlasov analysis by Okamoto and Yokoya [17], which also allowed for explicit analytical expressions for coherent frequencies.

Note that these parametric cases are instabilities, which are “pumped” from noise under a half-integer resonance condition with the periodic focusing. They require no initial nonlinearity and even exist for uniform density KV-distributions. An example for a 3D Gaussian short bunch simulation by the TRACEWIN code in a periodic FODO lattice is shown in Fig. 3 (see also Ref. [18]). The primarily excited mode is the coherent parametric instability of the envelope mode $m = 2; n = 1$ in Eq. 4 - commonly called envelope instability -, which requires Q_{xy} near the quarter integer. In a FODO lattice this amounts to a zero-current phase advance per cell $k_{0xy} > 90^\circ$, and simultaneously for the space charge depressed rms phase advance $\bar{k}_{xy} < 90^\circ$.

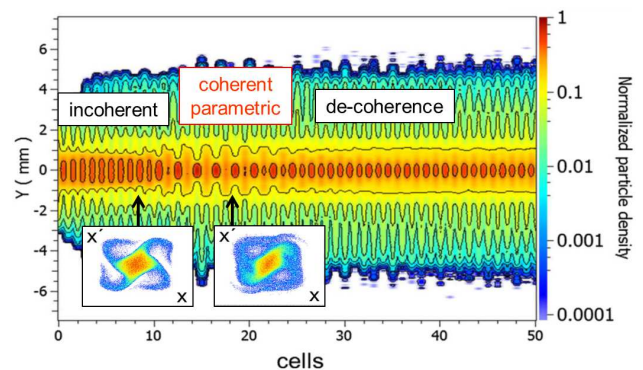


FIG. 3. Real space density evolution of a 3D high-intensity Gaussian bunch subject to parametric envelope instability in the 90° stopband of a FODO lattice ($k_{0xy} = 120^\circ$, $\bar{k}_{xy} = 73^\circ$) (source: Ref. [18]).

Fig. 3 shows the rapid evolution of an initial fourth order structure resonance phenomenon (note the four-fold symmetry insert of transverse phase space), which is driven by the periodic space charge pseudo octupole present in the Gaussian density profile and described by the incoherent resonance condition $4k_{xy} = 360^\circ$ following the lattice periodicity. This is followed by the second order half-integer parametric mode described by $2(\bar{k}_{xy} + F_2 \Delta \bar{k}_{xy}) = \frac{1}{2}$ (with $F_2 = \frac{1}{2}$ for the unsplit tunes in xy). Note that two lattice periods are needed to complete one period of the envelope instability. After more than rms emittance doubling the coherent mode de-coheres again and results in a beam distribution following again the lattice periodicity.

Theoretically, as predicted by the analytical theories of Refs. [16, 17] ignoring Landau damping, such coherent half-integer parametric modes exist in all orders. Kojima et al. [15] have suggested that for synchrotron resonance charts also these coherent half-integer modes need to be included. Such a step would double the number of lines compared with so far commonly used charts. This trig-

gered questions as to how realistic these lines are, if Landau damping was included (see also a comment [19] and reply [20] on this article).

In fact, examples of selfconsistent simulations in FODO lattices using waterbag beams show these half-integer parametric modes up to fourth order as demonstrated in Fig. 4 (compare also similar results in Refs. [11, 13, 15]). The simulations have been carried out with the TRACEWIN code using 128.000 particles. The situation

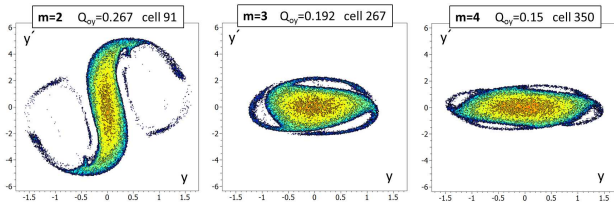


FIG. 4. Phase space projections for $m = 2, 3, 4; n = 1$ half-integer parametric modes and initial waterbag distribution ($\Delta\bar{Q}_{xy} = 0.0322$) (source: Ref. [13]).

is different for Gaussian distributions (truncated at 3σ): simulations in Ref. [11] for the same parameters shown that the third and fourth order modes are not excited. For these modes Landau damping works in transverse tune space with the necessary - not always sufficient - condition of a negative slope towards higher tunes, which also means higher amplitudes as shown schematically in Fig. 5. The exponentially growing parametric modes are damped, if there is an excess of particles at smaller frequencies (amplitudes). Apparently, the sharply truncated waterbag distribution lacks Landau damping for modes with a sufficiently large coherent shift, which is the case for all modes shown in the spectra of Fig. 2. The r.h.s. of Fig. 2 also shows that in case of $m = 2$

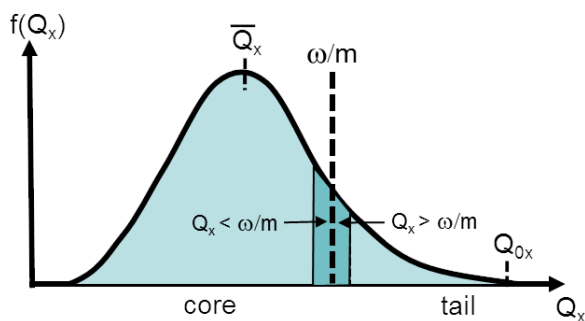


FIG. 5. Schematics of Landau damping of a coherent parametric mode with frequency ω in transverse tune space

there is only a weak overlap at the edge of the Gaussian tune spectrum, which apparently is not sufficient for Landau damping. In other words, the $m = 2$ mode is too strong to be damped by the small amount of particles near the edge.

The practical consequence following from the tune

spectra is our finding that for Gaussian distributions all coherent half-integer resonances are expected to be Landau damped, with the exception of the - in practical synchrotron lattice design less relevant - second order envelope instability case. This results in the important conclusion that the suggestion in Ref. [15] to add half-integer lines in resonance charts is not supported by theory in case of Gaussian-like distributions. Our Landau damping argument so far is valid for coasting beams, but it can be assumed that Landau damping is even further enhanced by the additional effect of synchrotron oscillations.

IV. INCOHERENT VERSUS COHERENT RESONANCES

Of practical importance is the interplay between coherent and incoherent resonance effects as described by Eq. 3. This subject has not been systematically explored in the context of high intensity synchrotrons, where long-term effects possibly raise the importance of incoherent resonance effects compared with coherent ones.

Unquestioned is the dominance of incoherent effects in the thin tail-halo region of a Gaussian-like distribution. Regarding incoherent effects in the denser beam core the discussion has been influenced by generalizing interpretations of earlier publications, which strongly emphasized the exclusive role of coherent effects in the core of a beam. The statement by Baartman [14] “In summary, we see the core is affected only by coherent core modes, and the tail affected by incoherent resonance” was originally intended for the special case of 1D sheet beams and short-term behavior of the $m = 2$ gradient error resonance.

This discussion is taken up again in the book by Ng [21] who finds “irrelevance of the incoherent tune” for resonances, except in the beam halo. It is unquestioned that these findings have some justification in the evolution of relatively short-term gradient error resonances. However, generalizing this discussion to all orders of resonances and the long-term behavior in synchrotrons - as recently postulated in Ref. [15] - needs more careful examination in a broader context.

In fact, as shown in Section III, Landau damping of the nonlinear coherent half-integer parametric resonances is a good example, where the incoherent spectrum of tunes comes into play with important consequences. For a more detailed discussion it is appropriate to include the tune space with the spectral distribution of tunes for a given phase space distribution instead of relying on short-term rms emittance evolution data. The importance of tune spectra is outlined in the following examples.

A first example of a sixth order resonance is indicated in Fig. 2 with the weak coupling resonance

$$2Q_x + 4Q_y = 1 \quad (5)$$

driven by the periodical pseudo-dodecapole space charge component of the matched beam. This resonance is a

local phenomenon involving only a very small neighborhood of tune space around the exact resonance condition. For this reason it is clearly an incoherent resonance. This is also reflected by the fact that it accurately satisfies Eq. 5 with no coherent shift term. Coherent resonances, on the other hand, may affect the beam even if the coherent resonance condition has *no overlap* with the tune footprint. This is, for example, the case for the waterbag beam $m = 2, 3, 4$ modes in Fig. 2.

Further evidence of an incoherent resonance occurring deeper in the beam core is demonstrated by lowering Q_{0y} such that the sixth order non-coupling resonance

$$6Q_y = 1 \quad (6)$$

is excited slightly below the edge of the Gaussian distribution (cut at 3σ), with the resulting phase space projection shown in Fig. 6. The incoherent resonance is effect-

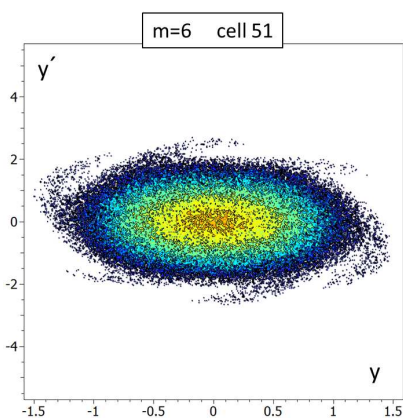


FIG. 6. Phase space projection in $y - y'$ (at cell 51) with $Q_{0y} = 0.184$ showing $m = 6$ incoherent integer resonance of Gaussian distribution.

ing the outer tail-halo region of the beam as expected. Note that the theoretically nearby coherent half-integer mode $m = 3; n = 1/2$ (following Eq. 4) is absent for a Gaussian due to Landau damping as discussed above.

For the slightly higher tune $Q_{0y} = 0.1875$ we show the tune spectrum on the l.h.s. graph of Fig. 7, and for $Q_{0y} = 0.1931$ in the r.h.s. graph. The incoherent resonance on the l.h.s. graph actually occurs almost at the upper edge of the tune spectrum, i.e. tail-halo region, and \bar{Q}_y far below the resonance at $Q_{xy} = 1/6$. It has - as expected - a pronounced effect by pushing quite a few particles above the resonance marked at $6Q_y = 1$. A 3% emittance growth occurs over 3000 cells of simulation, which apparently is still going on.

In the r.h.s. case of Fig. 7, \bar{Q}_y is still slightly below the resonance, but now deep in the beam core. Nonetheless particles are still shifted from below to above the resonance as indicated by the gap developing under it. The amount of resonant particles is much less than before, and the emittance growth only about 0.8%. We have also checked the still higher working point $Q_{0y} = 0.204$,

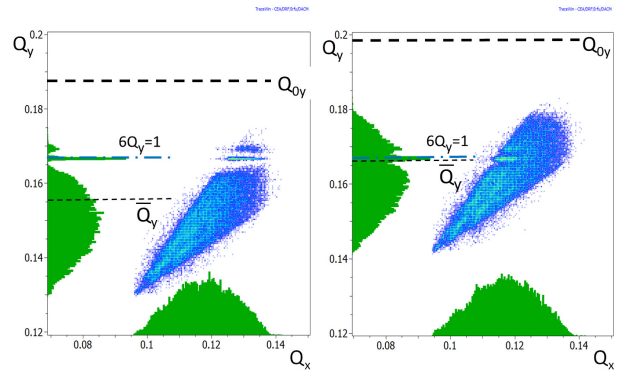


FIG. 7. Spectral distributions of Q_{xy} for Gaussian distributions at $Q_{0y} = 0.1875$ (l.h.s.) and $Q_{0y} = 0.1931$ (r.h.s.) showing the incoherent $6Q_y = 1$ resonance.

such that the resonance occurs below \bar{Q}_y and close to the maximum of the tune spectrum on the falling slope of it. In this case no effect of resonance could be detected. This supports the “rms tune” rule - also encountered in Section II and Refs. [8, 9] in the context of gradient error resonances - that no resonant effects should occur as long as \bar{Q}_y stays above the resonance line. This finding obviously merits further detailed research.

More long-term simulations, also including synchrotron oscillations, are a subject of future studies. Our point here is that the importance of incoherent resonances is not limited to the tail-halo region - as was suggested in Ref. [15] on the basis of simulations over some hundreds of cells only -, but they may also occur deeper in the core and contribute to emittance growth up to the spectral position of \bar{Q}_y . Also, we have not been able to detect any evidence of a coherent shift in this particular stopband as conjectured in Ref. [15], which also needs to be explored in a broader context.

V. COMPARISON WITH EXPERIMENTS

We suggest that these findings on incoherent resonances have a relevance for examining the validity of the FSM frozen space charge model. It has been used as relatively successful approximate simulation model to interpret experimental data on resonances with space charge in the CERN and GSI synchrotrons [3–5].

FSM simulation models only include incoherent resonance processes, while any coherent phenomena are suppressed due to the lack of selfconsistent feedback on the space charge potential. Obviously the credibility of FSM models gets weakened beyond the point, where significant changes in the distribution function or intensity occur. Nonetheless our findings on incoherent resonances lend support to the physics basis of FSM - up to some point.

In fact, the reported agreement between FSM simulations and experimental data looks better than one

might have expected in view of the lack of feedback. Results from the extended SIS18 benchmarking campaign at GSI [3] are shown in Fig. 8. Shown are the results of

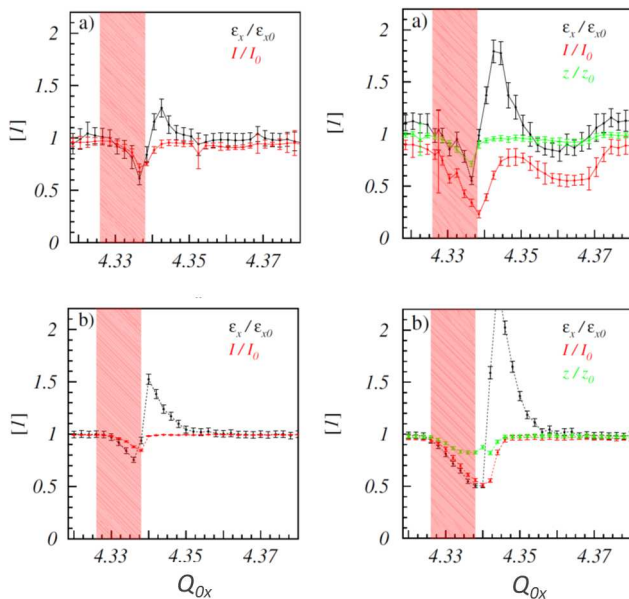


FIG. 8. Results of SIS18 measurements (a) and frozen space charge (FSM) simulations (b) near a sextupole error resonance at $Q_{0x} = 4.333$. Shown are relative changes of rms emittances and current versus the bare tune (here denoted by Q_x) for a coasting beam (left column) as well as for a bunched beam (right column). Also shown is the length change for the bunched beam. Source: Ref. [3].

measurements (upper row) and simulations (lower row) for a coasting (left column) and a bunched beam (right column). Rms emittance and beam loss have been obtained by scanning the working point across a horizontal third order error resonance given by $3Q_{0x} = 13$. Space charge is simulated for some 10^5 turns by adopting the FSM method for initial Gaussian beams consistent with measured profiles, and for a maximum tune shift $2\Delta Q_x = 0.025$ for the coasting, and $2\Delta Q_x = 0.04$ for the bunched beam.

Note the surprisingly good agreement of the measured and simulated data as far as center and width of stop-

bands. The conjecture of Section IV and Refs. [8, 9] that no emittance growth occurs as long as \bar{Q}_x is above the resonance is also surprisingly well reflected here: this amounts to $Q_{0x} > 4.35$ for the coasting, respectively $Q_{0x} > 4.36$ for the bunched beam case. Also note that the red hatched area in Fig.8 marks the stopband in the low intensity regime. The fact that the measured loss near this area is enhanced compared with simulations is attributed to the not sufficiently well-known dynamic aperture. This enhanced measured loss also limits the growth of rms emittances.

Altogether, comparison of measurements and FSM simulation justifies the preliminary interpretation that in long-term resonance response the incoherent resonance effects are the by far dominant mechanism. Coherent resonance effects, if noticeable, would have to show in Fig. 8 within the parameter regions $Q_{0x} < 4.35$ for the coasting, respectively $Q_{0x} < 4.36$ for the bunched beam case. There is, however, no evidence for this.

VI. OUTLOOK

Our discussion of incoherent space charge effects in transverse resonances has shown their significance in Landau damping of the coherent half-integer parametric resonances. In the absence of such damping they would justify the additional doubling of lines in resonance charts as suggested in Ref. [15]. It is expected that this equally applies to the - theoretically yet unexplored - selfconsistent behavior in bunched beams.

The role of coherent constituents in externally driven (integer type) resonances with space charge needs more quantitative research and benchmarking by simulation. However, we find that the small coherent shifts for higher than second order resonances - see Fig. 2 - are unlikely to have an important effect on the overall resonance response in case of long-term behavior. The discussion following Fig. 8 suggest that in long-term resonance dynamics they are most likely overshadowed by the incoherent effects.

In summary, emphasis of future work should be on long-term bunched beam simulation studies and code comparison for different types of resonances and strengths of space charge effects, and ideally in realistic synchrotron lattices.

-
- [1] L. Groening, W. Barth, W. Bayer, G. Clemente, L. Dahl, P. Forck, P. Gerhard, I. Hofmann, M. S. Kaiser, M. Maier, S. Mickat, and T. Milosic, D. Jeon and D. Uriot, Phys. Rev. Lett. **102**, 234801 (2009).
 - [2] L. Groening, I. Hofmann, W. Barth, W. Bayer, G. Clemente, L. Dahl, P. Forck, P. Gerhard, M. S. Kaiser, M. Maier, S. Mickat, T. Milosic, and S. Yaramyshev, Phys. Rev. Lett. **103**, 224801 (2009).
 - [3] G. Franchetti, O. Chorniy, I. Hofmann, W. Bayer, F. Becker, P. Forck, T. Giacomini, M. Kirk, T. Mohite, C. Omet, A. Parfenova, and P. Schütt, Phys. Rev. ST Accel. Beams **13**, 114203 (2010).
 - [4] G. Franchetti, S. Gilardoni, A. Huschauer, F. Schmidt, and R. Wasef, Phys. Rev. Accel. Beams **20**, 081006 (2017).
 - [5] H. Bartosik, Challenges in understanding space charge effects, *61st ICFA ABDW on High-Intensity and High-Brightness Hadron Beams (HB2018)*, Daejeon, Korea

- (JACOW, Geneva 2018) MOA1PL01 (2018).
- [6] L. Smith, Effect of gradient errors in the presence of space charge forces, in Proc. of the 4th Intern. Conf. on High-Energy Accelerators, edited by A. A. Kolomenskij and A. B. Kuznetsov (Dubna, USSR, 1963), p. 1232.
- [7] F. J. Sacherer, Ph.D thesis, Lawrence Radiation Laboratory Report No. UCRL-18454, 1968.
- [8] S. Machida, Space charge effects in low-energy proton synchrotrons, Nucl. Instrum. Methods Phys. Res., Sect. A **309**, 43 (1991).
- [9] H. Hotchi, H. Harada, N. Hayashi, M. Kinsho, K. Okabe, P.K. Saha, Y. Shobuda, F. Tamura, K. Yamamoto, M. Yamamoto and M. Yoshimoto, J-PARC 3-GeV RCS: 1-MW beam operation and beyond, JINST 15, P07022 (2020).
- [10] I. Hofmann, Stability of anisotropic beams with space charge, Phys. Rev. E **57**, 4713 (1998).
- [11] I. Hofmann, *Space Charge Physics for Particle Accelerators* (Springer, New York, 2017).
- [12] D. Uriot and N. Pichoff, in *Proceedings of IPAC2015*, Richmond, VA, USA (JACoW, Virginia, 2015), paper MOPWA008.
- [13] I. Hofmann, Revisiting coherent and incoherent resonances with space charge, JINST 15, P07022 (2020).
- [14] R. Baartman, Betatron resonances with space charge, *Proceedings of Space Charge Physics in High Intensity Hadron Rings*, Shelter Island, New York, USA, 1998, AIP Conf. Proc. **448**, 56 (1998).
- [15] K. Kojima, H. Okamoto, and Y. Tokashiki, Empirical condition of betatron resonances with space charge, Phys. Rev. Accel. Beams **22**, 074201 (2019).
- [16] I. Hofmann, L.J. Laslett, L. Smith and I. Haber, Stability of the Kapchinskij-Vladimirskij (K-V) distribution in long periodic transport systems, Part. Accel. **13** 145 (1983).
- [17] H. Okamoto and K. Yokoya, Parametric resonances in intense one-dimensional beams propagating through a periodic focusing channel, Nucl. Instrum. Methods Phys. Res., Sect. A **482**, 51 (2002).
- [18] I. Hofmann and O. Boine-Frankenheim, Parametric instabilities in 3D periodically focused beams with space charge, Phys. Rev. Accel. Beams **20**, 014202 (2017).
- [19] I. Hofmann, Comment on “Empirical condition of betatron resonances with space charge”, Phys. Rev. Accel. Beams, **23**, 028001 (2020).
- [20] K. Kojima, H. Okamoto, and Y. Tokashiki, Reply to “Comment on ‘Empirical condition of betatron resonances with space charge’”, Phys. Rev. Accel. Beams **23**, 028002 (2020).
- [21] K. Y. Ng, Physics of intensity dependent beam instabilities (World Scientific, Singapore, 2005).